

Triton Electric Form Factor at Low-Energies

H. Sadeghi*

Department of Physics, University of Arak, P.O.Box 38156-879, Arak, Iran.

Abstract

Making use of the Effective Field Theory(EFT) expansion recently developed by the authors, we compute the charge form factor of triton up to next-to-next-to-leading order (N²LO). The three-nucleon forces(3NF) is required for renormalization of the three-nucleon system and its effects are predicted for process and is qualitatively supported by available experimental data. We also show that, by including higher order corrections, the calculated charge form factor and charge radius of ³H are in satisfactory agreement with the experimental data and the realistic Argonne v_{18} two-nucleon and Urbana IX potential models calculations. This method makes possible a high precision few-body calculations in nuclear physics. Our result converges order by order in low energy expansion and also cut-off independent.

PACS numbers: 21.45.+v, 25.10.+s, 25.20.-x, 27.10.+h

keywords: effective field theory, three-body system, three-body force, triton form factor

arXiv:0908.2052v1 [nucl-th] 14 Aug 2009

*Electronic address: H-Sadeghi@araku.ac.ir

I. INTRODUCTION

The few-body problem has now reached the stage when the main interest is centered not on theoretical techniques but on the application of these techniques to problems in nuclear, particle and atomic physics. Among these theories, EFT is a powerful tool to calculate low-energy observables in a systematic way. Pionless EFT has been applied to two- and three-nucleon systems [1, 2, 3, 4, 5, 6, 7, 8, 9], during the last few years. It is ideally suited to exploit a separation between scales and can use with contact interactions at low-energies. Some of these low-energy observables such as neutron-deuteron radiative capture and the two-body photodisintegration of the triton have been calculated using pionless EFT and insertion of the three-body force, up to $N^2\text{LO}$ [10, 11, 12, 13]. In these calculation we find a simple way for inclusion of external currents. The evaluated cross sections have been compared with experimental data and other modern realistic two- and three-nucleon forces AV18/UrbIX potential models calculations. We are also going to study the structural functions of three-body systems in future calculations. Among them, the study of the three-body nuclear physics involving the charge form factors and charge radius of ^3H is calculated by using pionless EFT. It have been investigated in theoretical and experimental works over the past decays.

The effect of meson exchange currents on the charge and magnetic form factors of ^3H was investigated by Maize et al. [14] and ref there in. Inclusion of meson exchange currents considerably improves the impulse approximation fits to the experimental data. An other calculation reported in include single- Δ isobar admixtures in the three-nucleon wave function [15].

Recently, a very good agreement reached with the calculation of the charge form factor of ^3H [16, 17]. They calculated the electromagnetic form factors of the three-nucleons ^3H with wave functions obtained with the Argonne v18 two-nucleon and Urbana IX three-nucleon interactions. The two-body currents required by current conservation with the v18 interaction as well as those associated with $N\Delta$ transition currents and the currents of Δ resonance components in the wave functions, are considered for these calculations. In this way, explicit three-nucleon current operators associated with the two-pion exchange three-nucleon interaction arising from irreducible S-wave pion-nucleon scattering is constructed and it is shown to have very little effect on the calculated magnetic form factors.

More recent calculation of the triton charge form factor at leading order in $\ell/|a|$ and extract the charge radius has been performed by Platter et al. [18]. They studied the correlation between the triton binding energy and charge radius and relate it to the three-body parameter L_3 that parameterizes the Phillips and Tjon lines in effective theory.

In experimental works, the ^3H charge form factor was measured in the range $0.29 < q^2 < 1 \text{ fm}^{-2}$ by Beck et al. [19]. After few years, the charge and magnetic form factors were also measured in the range $0.0477 < q^2 < 2.96 \text{ fm}^{-2}$ [20]. The experimental result of triton charge radius is quoted as $r_c = 1.63 \pm 0.03 \text{ fm}$ [20]; as $r_c = 1.76 \pm 0.04 \text{ fm}$ [22]; as $r_c = 1.81 \pm 0.05 \text{ fm}$ [23]; and as $r_c = 1.755 \pm 0.086 \text{ fm}$ [24].

In this paper, we study the charge form factor and charge radius of the triton to next-to-next-to-leading order ($N^2\text{LO}$). Our results show that, by including higher order corrections, the calculated charge form factor of ^3H is in satisfactory agreement with the modern nucleon-nucleon potential AV18 together with the three- nucleon force UrbanaIX. This result has several implications. The first and most important one is the remarkable success of EFT improving for simple inclusion of external currents. The second is the indication that the model makes possible a high precision three-body calculations in nuclear physics. It now appears to explain the structural functions of three-body systems. The third

is remarkable quality of the EFT low-energy calculations. The result converges order by order in low energy expansion, model independent and also cut-off independent. It should be considered that it is a quantitative question based on current choices and gauge invariance of nuclear force models to reveal signatures by switching on and off 3N forces.

This paper is divided into five main sections. Section II contains a brief description of the calculation of the the bound three-body systems. Faddeev integral equation, Lagrangian and kernel for the reaction involved in our consideration and three-body forces are given in this section. In Section III, we calculate the charge form factor of the triton by using EFT. Calculation of the charge form factors, the relevant diagrams, and parameters are discussed in this section. In section IV, comparisons of our results with the corresponding experimental and theoretical data are given. Finally section V contains a concluding discussion.

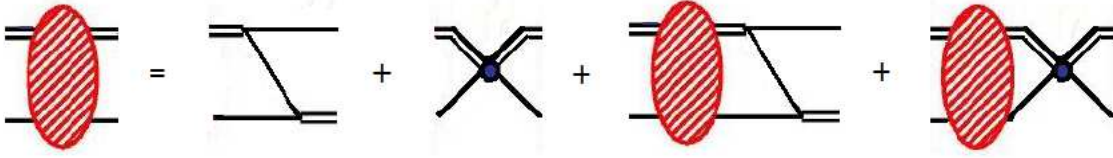


FIG. 1: Faddeev equation for the three-body amplitude including the three-body force. Line shows nucleon and thick solid line is propagator of the two intermediate auxiliary fields d_s and d_t . The three-body interactions with strength \mathcal{H} , denoted by the dot.

II. BRIEF REVIEW OF THE BOUND THREE-BODY SYSTEM

The derivation of the integral equation describing neutron-deuteron scattering has been widely discussed [5, 9]. We present here only the result, including the new term generated by the two-derivative three-body force. The three-nucleon lagrangian is given by [6]:

$$\begin{aligned} \mathcal{L} = & N^\dagger \left(i\partial_0 + \frac{\nabla^2}{2M} \right) N + d_s^{A\dagger} \left(-i\partial_0 - \frac{\nabla^2}{4M} + \Delta_s \right) d_s^A + d_t^{i\dagger} \left(-i\partial_0 - \frac{\nabla^2}{4M} + \Delta_t \right) d_t^i \\ & + t^\dagger \left(i\partial_0 + \frac{\nabla^2}{6M} + \frac{\gamma^2}{M} + \Omega \right) t - g_s \left(d_s^{A\dagger} (N^T P^A N) + \text{H.c.} \right) - g_t \left(d_t^{i\dagger} (N^T P^i N) + \text{H.c.} \right) \\ & - \omega_s \left(t^\dagger (\tau^A N) d_s^A + \text{H.c.} \right) - \omega_t \left(t^\dagger (\sigma^i N) d_t^i + \text{H.c.} \right) + \dots, \end{aligned} \quad (1)$$

where N is the nucleon iso-doublet and the auxiliary fields t , d_s^A and d_t^i carry the quantum numbers of the ${}^3\text{H}$ spin and isospin doublet, 1S_0 di-nucleon and the deuteron, respectively. The projectors are $P^i = \frac{1}{\sqrt{8}}\tau_2\sigma_2\sigma^i$ and $P^A = \frac{1}{\sqrt{8}}\sigma_2\tau_2\tau^A$, where $A = 1, 2, 3$ and $i = 1, 2, 3$ are iso-triplet and vector indices and τ^A (σ^i) are isospin (spin) Pauli matrices.

For calculation in this channel, two amplitudes get mixed (see fig. 1): t_s describes the $d_t + N \rightarrow d_s + N$ process, and t_t describes the $d_t + N \rightarrow d_t + N$ process:

$$\begin{aligned}
t_s(p, k) &= \frac{1}{4} [3\mathcal{K}(p, k) + 2\mathcal{H}(E, \Lambda)] + \frac{1}{2\pi} \int_0^\Lambda dq q^2 [\mathcal{D}_s(q) [\mathcal{K}(p, q) + 2\mathcal{H}(E, \Lambda)] t_s(q) \\
&\quad + \mathcal{D}_t(q) [3\mathcal{K}(p, q) + 2\mathcal{H}(E, \Lambda)] t_t(q)] \\
t_t(p, k) &= \frac{1}{4} [\mathcal{K}(p, k) + 2\mathcal{H}(E, \Lambda)] + \frac{1}{2\pi} \int_0^\Lambda dq q^2 [\mathcal{D}_t(q) [\mathcal{K}(p, q) + 2\mathcal{H}(E, \Lambda)] t_t(q) \\
&\quad + \mathcal{D}_s(q) [3\mathcal{K}(p, q) + 2\mathcal{H}(E, \Lambda)] t_s(q)] \quad , \quad (2)
\end{aligned}$$

with

$$\begin{aligned}
\mathcal{D}_s(q) &= \frac{1}{-\gamma_s + \sqrt{\frac{3}{4}(q^2 - k^2) + \gamma_t^2}} + \\
&\quad + \frac{3r_s}{8} \frac{q^2 - k^2 + \frac{4}{3}\gamma_t^2}{\left(-\gamma_s + \sqrt{\frac{3}{4}(q^2 - k^2) + \gamma_t^2}\right)^2} + \left(\frac{3r_s}{8}\right)^2 \frac{(q^2 - k^2 + \frac{4}{3}\gamma_t^2)^2}{\left(-\gamma_s + \sqrt{\frac{3}{4}(q^2 - k^2) + \gamma_t^2}\right)^3} . \quad (3)
\end{aligned}$$

where $\mathcal{D}_{s,t}(q) = \mathcal{D}_{s,t}(E - \frac{q^2}{2M}, q)$ are the propagators of deuteron.

For the spin-triplet S-wave channel, one replaces the two boson binding momentum γ and effective range ρ by the deuteron binding momentum $\gamma_t = 45.7025$ MeV and effective range $\rho_t = 1.764$ fm. Because there is no real bound state in the spin singlet channel of the two-nucleon system, its free parameters are better determined by the scattering length $a_s = 1/\gamma_s = -23.714$ fm and the effective range $r_s = 2.73$ fm at zero momentum, The neutron-deuteron $J = 1/2$ phase shifts δ is determined by the on-shell amplitude $t_t(k, k)$, multiplied with the wave function renormalization [6].

$$T(k) = Z t_t(k, k). \quad (4)$$

In that case, a unique solution exists in the $^2S_{1/2}$ -channel for each Λ and vanishing three-body force, but no unique limit as $\Lambda \rightarrow \infty$. As long distance, phenomena must however be insensitive to details of the short-distance physics (and in particular of the regulator chosen), Bedaque et al. [6, 9] showed that the system must be stabilized by introducing of a three-body force in a form:

$$\mathcal{H}(E; \Lambda) = \frac{2}{\Lambda^2} \sum_{n=0}^{\infty} H_{2n}(\Lambda) \left(\frac{ME + \gamma_t^2}{\Lambda^2} \right)^n. \quad (5)$$

which absorbs all dependence on the cutoff as $\Lambda \rightarrow \infty$ [6]. At leading order, $\gamma \ll \Lambda$, the essential observation are of order $\mathcal{O}(Q/\Lambda)$ and are independent of energy (or momentum) and hence can be made to vanish by only H_0 and not any of the higher derivative three-body forces. At NLO, there is only a perturbative change from the LO asymptotic of order $\mathcal{O}(1/\Lambda^2)$ (see [6]).

For N²LO order, a new three-body force seems to be required. The terms will be proportional to ME arising from expanding the kernel in powers of q/Λ and \sqrt{ME}/Λ and a three-body force term which contains a dependence on the external momenta k^2 and ME can absorb them. It means we need H_2 for calculations up to N²LO. It has been shown that the three-body system at N²LO can be renormalized without the need for an energy dependent three-body force at this order [8].

In the presence of an electromagnetic interactions, after performing minimal substitution, requires that ∇ operators be replaced by covariant derivatives $\mathbf{D} = \nabla - ie\mathbf{A}$, and time-derivatives ∂_0 be replaced by $D_0 = \partial_0 + ieA_0$ in lagrangian eq. (1), where \mathbf{A} is the vector potential.

This simple perturbative expansion of the scattering amplitude is reproduced order by order in the pionless expansion. Relativistic corrections are encountered at N²LO and effective range expansion provides a complete description of scattering in the low-energy region[6].

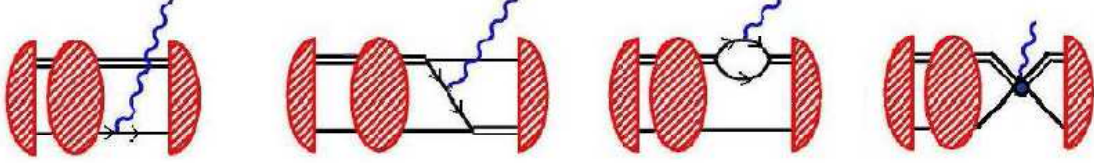


FIG. 2: Diagrams that contribute to the triton charge form factor. Wavy line shows photon. Remaining notation as in fig. 1.

III. THE CHARGE FORM FACTOR OF TRITON

The electric charge form factor of the triton is measured over a wide range of momentum transfers. The modern nucleon-nucleon potential AV18 together with the three-nucleon force UrbanaIX potential models and effective theory reproduce the data very well in the kinematic regions where they are applicable. (For a recent review, see [17, 18].). In present work, we calculate the charge form factor in the range $0 < q^2 < 0.3 \text{ fm}^{-2}$ in corresponding to recent effective theory calculation [18].

A convenient expression to calculate the charge form factors of a J=1/2 nucleus, such as the triton, is obtained by the matrix element of the electric current, is given by:

$$\langle \Psi_+ | J_e | \Psi_+ \rangle = e F_C(q^2) \quad , \quad (6)$$

where \mathbf{q} is the momentum transfer and Ψ_+ is the normalized ground state wave function. The dimensionless charge form factor defined in eq. (6) are normalized such that $F_C(0) = 1$. The slope of the charge form factor at low-momentum transfer defines the triton charge radius:

$$F_C(\mathbf{q}^2) = 1 - \mathbf{q}^2 \langle r^2 \rangle / 6 + \dots \quad (7)$$

where $r_C \equiv \langle r^2 \rangle^{1/2}$ is the charge radius.

In the pionless EFT, the charge form factor $F_C(q^2)$ has an expansion in powers of Q , $F_C(q^2) = F_C^{(0)}(q^2) + F_C^{(1)}(q^2) + F_C^{(2)}(q^2) + \dots$, where the superscript denotes the order of the contribution.

The diagrams that contribute to the deuteron charge form factor in pionless EFT are shown in fig. 2. In addition to diagrams where the photon couples to the nucleon, there are also couplings to the dibarion field obtained by gauging the Lagrange density in eq. (1).

The LO order calculation is corresponding to the leading term in a effective range expansion and is in corresponding with the charge form factor computed in ref. [18]. At higher orders there are contributions from higher dimension operators involving more derivatives on the nucleon field, such as

the nucleon charge radius operator, and also from higher dimension couplings of the dibaryon field, that is the dibaryon charge radius. At NLO, we have contributions coming only from insertions of the kinetic energy in the deuteron propagator. The NLO corrections to neutron-deuteron scattering are simply the range corrections in first order perturbation theory.

At N²LO order there will be corrections to neutron-deuteron scattering which are simply two times insertions of the kinetic energy in the deuteron propagator as well as correction from nucleon structure comes from the nucleon radii[2, 3]. For higher orders in the EFT expansion, order Q^3 , there are contributions from several types of graphs, including relativistic corrections and contribution from, a four-nucleon-one-photon operator, the dibaryon charge radius operator.

The last diagram also show the photon couples to the three-nucleon force. At LO calculation, there is no interaction of \mathbf{H}_0 with a photon, because H_0 has no derivatives, so it is not affected by the minimal substitution $\mathbf{P} \rightarrow \mathbf{P} - e\mathbf{A}$. In other hand, contribution from the photon couples to the three-nucleon field (\mathbf{H}_2) is calculated at N²LO.

Low-energy observables must be independent of an arbitrary regulator Λ up to the order of the expansion. One can therefore estimate sensitivity of the results to cut-off Λ , and hence provide a reasonable error-analysis, by employing a momentum cut-off in the solution of the Faddeev equation and varying it between the breakdown-scale Λ_π and ∞ . The cut-off varied between $\Lambda = 200$ MeV and $\Lambda = 550$ MeV.

IV. RESULTS AND DISCUSSION

A numerical solution of the charge form factor and charge radius of triton have been done. The numerical values and parameters used for calculation is described in ref. [11]. We solved integral equation by insertion of Q in Faddeev equation where is shown in figs. 1 and 2. The integral equation is solved by the first two terms of the effective range expansion, properly iterating and folding to electromagnetic interaction where are shown in fig. 2 order by order and integrated on the involving momentum. The three-body parameter \mathbf{H}_0 is fixed from the $^2S_{1/2}$ scattering length $a_3 = (0.65 \pm 0.04)$ fm at LO. \mathbf{H}_2 is also required at N²LO and it is determined by the triton binding energy $B_3 = 8.48$ MeV.

The calculated ^3H charge form factor is compared with the experimental data. The results have been shown in fig. 3. The rhomboids and squares are experimental data from Refs. [21] and [19], respectively. While the general trend of the low-momentum transfer form factor data is reproduced by our calculation, we obtain a somewhat close slope to the experiments up to N²LO. The remarkable success of the present calculation by using EFT should be stressed. The number of three-body calculations with external currents is however, extremely limited. It suggests, in particular, that the present model provide simple inclusion of external currents. Yet, the excellent agreement between the calculated and measured results of charge form factor suggests that these corrections may be negligible.

Finally, values for the charge radii of ^3H are listed in Table I. The results in comparison of the modern nucleon-nucleon potential AV18 together with the three- nucleon force UrbanaIX, are found to be in good agreement with experimental data. Fitting a polynomial in \mathbf{q}^2 to our result for the charge form factor, eq.(7), we can extract the triton charge radius. This procedure leads to a triton charge radius $r_c = [1.959(\text{LO}) - 0.113(\text{NLO}) - 0.071(\text{N}^2\text{LO})]\text{fm} = [1.775 \pm 0.02]\text{ fm}$.

The cut-off variation has been also done. These variations were nearly independent of variation of momentum and decreased steadily when the order of calculation is increased up to N²LO.

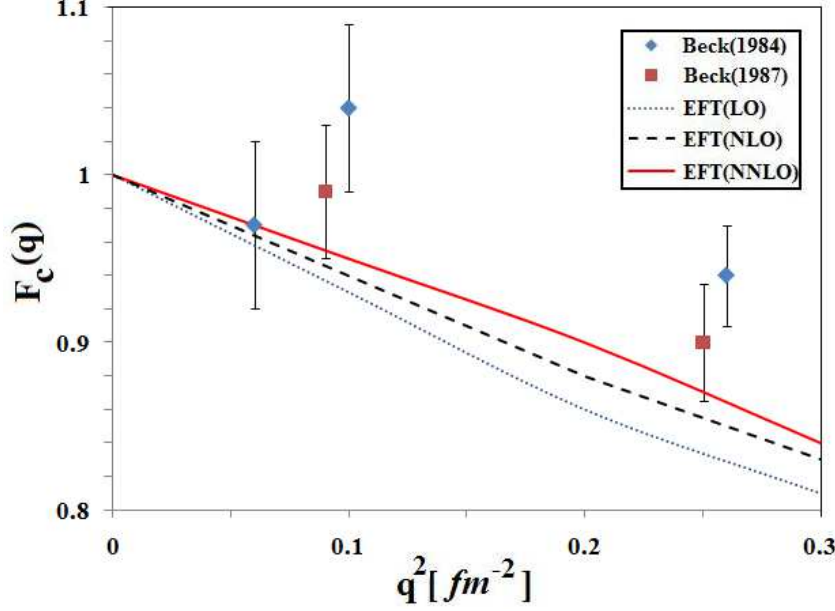


FIG. 3: The triton charge form factor. Dot, dash and solid curve are LO, NLO, and N²LO EFT results. The rhomboids and squares are experimental data from Refs. [20] and [21], respectively.

TABLE I: Comparison between different theoretical and experimental results for triton charge radius in fm.

Theory	Triton charge radius	% Error
Effective theory [18]	2.1	20
Argonne v18+Urbana IX [17]	1.722	2
Argonne v18+Urbana IX [16]	1.725	2
EFT(LO)	1.959	12
EFT(NLO)	1.846	5
EFT(N ² LO)	1.775	1.1
Exp. [24]	1.755±0.086	

In fig. 4, we show the correlation between the triton charge radius and binding energy of triton. The solid line denotes leading order effective theory result [18]. The two boxes show modern calculations (including meson exchange currents) based on the AV18 potential with and without the Urbana IX three-body force [17]. The circles indicate Faddeev calculations using different potentials from Refs. [25, 26]. The correlation curve of Ref. [27] is given by the dotted line. The triangle with error-bar indicates the experimental values [24]. Short-dash, dot-dash and long-dash curves are LO, NLO, and N²LO our EFT results, respectively. It should be considered that the inclusion of the range correction moves the universal line closer to the experimental values in corresponding to Phillips line.

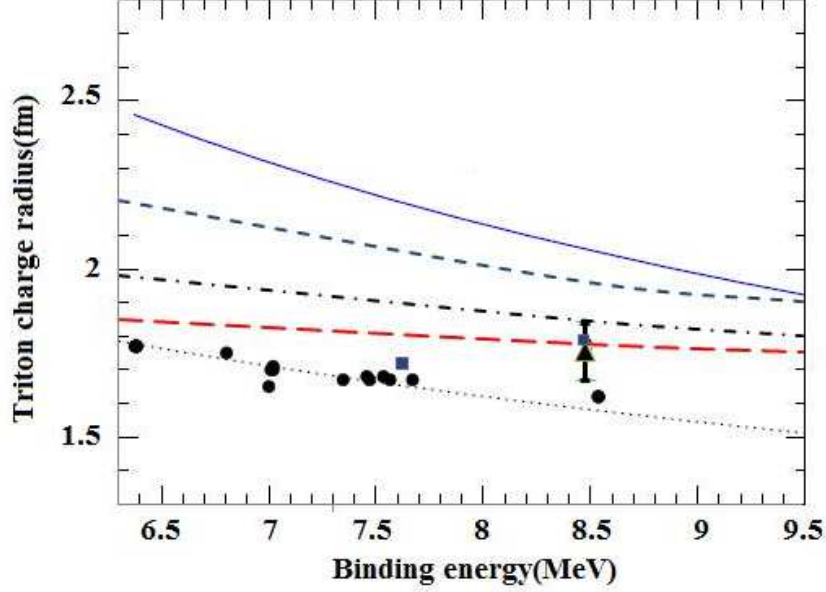


FIG. 4: The correlation between the triton charge radius and binding energy. The solid line denotes leading order effective theory result [18]. The circles indicate Faddeev calculations using different potentials from Refs. [25, 26] while the two boxes show modern calculations using AV18 with and without the Urbana IX three-body force [17]. The correlation curve of Ref. [27] is given by the dotted line. The triangle with error-bar indicates the experimental values [24]. Short-dash, dot-dash and long-dash curves are LO, NLO, and N^2 LO our EFT results, respectively. For better comparison, axes scales are chosen like as [18].

V. SUMMERY AND CONCLUSION

The goal of this work was to obtain the charge form factor and charge radius of triton, as a three-body bound state, that are obtained by using EFT. We applied the formalism developed to the computation of processes involving external currents such as, triton charge form factor and charge radii. We considered the diagrams needed to be computed and the charge form factor numerically obtained by perturbatively solving of Faddeev equation, up to N^2 LO. At very low energies, the interactions between nucleons can be only described by point-like interactions. The present study of the triton charge form factor show that it is possible to obtain remarkably good predictions for electrogenic structure functions of the few-body bound states by using EFT at very low-energies.

The charge form factor of triton at low energies was calculated by using pionless EFT and simple inclusion of external currents. The charge radii is also calculated up to N^2 LO. The triton binding energy and nd scattering length in the triton channel have been used to fix them. Hence the triton charge radii is in total determined as $r_c = [1.959(\text{LO}) - 0.113(\text{NLO}) - 0.071(\text{N}^2\text{LO})]\text{fm} = [1.775 \pm 0.02]\text{fm}$. It converges order by order in low energy expansion and is also cut-off independent at this order. The results also move the universal line closer to the experimental values when order of calculation increases. This is in corresponding to the Phillips line.

VI. ACKNOWLEDGMENTS

The author would like to thank H.W. Griesshammer for many helpful discussions and his available mathematica code. This work is supported in part by the university of Arak.

-
- [1] D. B. Kaplan, M. J. Savage and M. B. Wise, Nucl. Phys. B **534**, (1998) 329.
 - [2] J.-W. Chen, G. Rupak, and M. J. Savage, Nucl. Phys. A **653**, (1999) 386.
 - [3] S. R. Beane and M. J. Savage, Nucl. Phys. A **694**, (2001) 511.
 - [4] P. F. Bedaque, H.-W. Hammer and U. van Kolck, Phys. Rev. Lett. **82**, (1999) 463; Nucl. Phys. A **646**, (1999) 444.
 - [5] P. F. Bedaque, H.-W. Hammer and U. van Kolck, Nucl. Phys. A **676**, (2000) 357.
 - [6] P. F. Bedaque, G. Rupak, H. W. Griesshammer and H.-W. Hammer, Nucl. Phys. A **714**, (2003) 589.
 - [7] F. Gabbiani, P. F. Bedaque and H. W. Griesshammer, Nucl. Phys. A **675**, (2000) 601.
 - [8] L. Platter and D. R. Phillips, Few Body Syst. **40**, (2006) 35.
 - [9] H.W. Griesshammer, Nucl. Phys. A **760**, (2005) 110.
 - [10] H. Sadeghi and S. Bayegan, Nucl. Phys. A **753**, (2005) 291.
 - [11] H. Sadeghi, S. Bayegan and H. W. Griesshammer, Phys. Lett. B **643**, (2006) 263.
 - [12] H. Sadeghi, Phys. Rev. C **75**, (2007) 044002.
 - [13] H. Sadeghi, Submitted for publication.
 - [14] M.A. Maize and Y.E. Kim, Nucl. Phys. A **420**, (1984) 365; Errata, Nucl. Phys. A **443**, (1985) 747.
 - [15] W. Struensee, Ch. Hajduk, P.U. Sauer and W. Theis, Nucl. Phys. A **465**, (1987) 651.
 - [16] L.E. Marcucci, D.O. Riska and R. Schiavilla, Phys. Rev. C **58**, (1998) 3069.
 - [17] J. Golak, et al., Phys. Rept. **415**, (2005) 89.
 - [18] L. Platter and H.-W. Hammer, Nucl. Phys. A **766**, (2006) 132.
 - [19] D.H. Beck, J. Asai and D.M. Skopik, Phys. Rev. C **25**, (1982) 1152.
 - [20] D.H. Beck, et al., Phys. Rev. C **30**, (1984) 1403.
 - [21] D. Beck et al., Phys. Rev. Lett **59**, (1987) 1537.
 - [22] F.-P. Juster, et al., Phys. Rev. Lett **55**, (1985) 2261.
 - [23] J. Martino, Lect. Notes in phys. **260**, (1986) 129.
 - [24] A. Amroun et al., Nucl. Phys. A **579**, (1994) 596.
 - [25] G.L. Payne, J.L. Friar, B.F. Gibson, and I.R. Afnan, Phys. Rev. C **22**, (1980) 823.
 - [26] C.R. Chen, G.L. Payne, J.L. Friar, and B.F. Gibson, Phys. Rev. C **31**, (1985) 2266.
 - [27] J.L. Friar, B.F. Gibson, C.R. Chen, and G.L. Payne, Phys. Lett. B **161**, (1985) 241.